Transp Porous Med (2012) 95:337–348
DOI 10.1007/s11242-012-0046-5

A Numerical Study of Oscillating Peristaltic Flow of Generalized Maxwell Viscoelastic Fluids Through a Porous Medium

Dharmendra Tripathi · O. Anwar Bég

Received: 28 February 2012 / Accepted: 6 July 2012 / Published online: 25 July 2012

Abstract This article presents a numerical study on oscillating peristaltic flow of generalized Maxwell fluids through a porous medium. A sinusoidal model is employed for the oscillating flow regime. A modified Darcy-Brinkman model is utilized to simulate the flow of a generalized Maxwell fluid in a homogenous, isotropic porous medium. The governing equations are simplified by assuming long wavelength and low Reynolds number approximations. The numerical and approximate analytical solutions of the problem are obtained by a semi-numerical technique, namely the homotopy perturbation method. The influence of the dominating physical parameters such as fractional Maxwell parameter, relaxation time, amplitude ratio, and permeability parameter on the flow characteristics are depicted graphically. The size of the trapped bolus is slightly enhanced by increasing the magnitude of permeability parameter whereas it is decreased with increasing amplitude ratio. Furthermore, it is shown that in the entire pumping region and the free pumping region, both volumetric flow rate and pressure decrease with increasing relaxation time, whereas in the co-pumping region, the volumetric flow rate is elevated with rising magnitude of relaxation time.

Keywords Oscillating flow · Peristalsis · Trapping · Fractional Maxwell model · Porous medium · Homotopy perturbation method (HPM) · Pumping

1 Introduction

Non-Newtonian characteristics are exhibited by numerous fluids including *physiological liquids* (blood, food bolus, chime, bile etc.), *geological suspensions* (drilling muds, sedimentary liquids), *industrial tribological liquids* (oils and greases), and *biotechnological liquids* (biodegradable polymers, gels, food stuffs etc.). It is difficult to propose a single model which

D. Tripathi (✉)
Department of Mathematics, Indian Institute of Technology Ropar, Rupnagar, 140001 Punjab, India
e-mail: dtripathi.rs.apm@itbhu.ac.in

O. A. Bég
Biomechanics Research, Aerospace Engineering, Department of Engineering and Mathematics, Sheffield Hallam University, Sheffield, S11WB, UK

can exhibit all the properties of non-Newtonian fluids. To describe the viscoelastic properties of such fluids, recently, constitutive equations with *ordinary* and *fractional time derivatives* have been introduced. Fractional calculus has proved to be very successful in the description of constitutive relations of viscoelastic fluids. The starting point of the fractional derivative model of viscoelastic fluids is usually a *classical differential equation* which is modified by replacing the time derivative of an integer order with fractional order and may be formulated both in the *Riemann–Liouville* or *Caputo sense* (see Mainardi and Spada 2011). This generalization allows one to define precisely *non-integer order integrals* or *derivatives*. Considering the relevance of fractional models of viscoelastic fluids, a number of articles (Tan et al. 2003; Qi and Jin 2006; Vieru et al. 2008; Wang and Xu 2009; Khan et al. 2009a,b,c, 2010; Khan 2009a,b; Qi and Xu 2009; Nadeem 2007; Liu et al. 2011) have addressed unsteady flows of viscoelastic fluids in conduits with the fractional Maxwell model, fractional generalized Maxwell model, fractional second grade fluid, fractional Oldroyd-B model, fractional Burgers' model, or fractional generalized Burgers' model for a variety of different geometries for the wall surface. Solutions for the velocity field and the associated shear stress in such studies have frequently been obtained by using various transforms including the Laplace transform, Fourier transform, Weber transform, Hankel transform, or discrete Laplace transform methods.

Oscillating (or transient) flow of non-Newtonian fluids through a channel or tube is a fundamental flow regime encountered in many biological and industrial transport processes. The quasi-periodic blood flow in the cardiovascular system, movement of food bolus in the gastrointestinal tract and urodynamic transport in the human ureter are just several examples of oscillating flow in biological systems. Industrial applications of oscillating flows include slurry and waste conveyance systems employing roller pumps and finger pumps. The low Reynolds numbers characterizing such flows, and the fact that, the dimensions of the channels and macromolecules in the fluid can be of the same order of magnitude, can lead to effects unseen in macroscopic systems. As such fractional models have been studied extensively in recent years in biomedical transport problems. Tripathi et al. (2010) investigated the peristaltic flow of a fractional Maxwell fluid through a channel. Further studies have utilized the generalized fractional Maxwell model, fractional Oldroyd-B model, and fractional Burgers' model (Tripathi 2011a,b,c,d,e,f; Tripathi et al. 2011; Tripathi 2011g) in a variety of peristaltic flow configurations. Some semi-numerical and analytical methods including the homotopy perturbation method (HPM), homotopy analysis method (HAM), variational iteration method (VIM), and Adomian decomposition method (ADM) have been employed to obtain robust solutions of fractional partial differential equations (FPDE).

To the best knowledge of the authors, no studies thus far have examined analytically the oscillating flow of *generalized Maxwell fluids* through a porous medium. In this study, we therefore study this case and furthermore employ the *HPM* to derive approximate analytical solutions of this problem. Numerical results for different cases are depicted graphically. Peristaltic flow patterns have been visualized with Mathematica software. The influences of fractional parameter, relaxation time, and permeability parameter on the oscillating peristaltic flow pattern are discussed in detail. This study is relevant to transport in biomechanical systems where porous media and oscillating flows often arise.

2 Mathematical Model

The constitutive equation for the shear stress–strain relationship of viscoelastic fluids obeying the fractional Maxwell model (Mainardi and Spada 2011; Xue and Nie 2008) is given by:

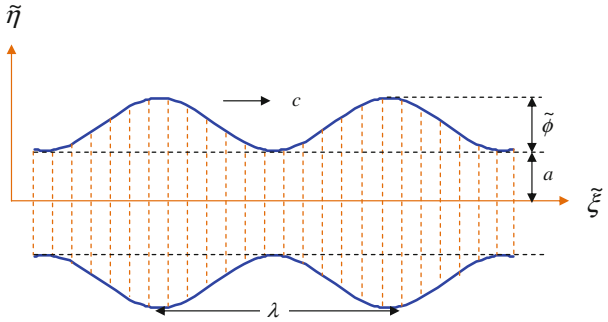

Fig. 1 Geometry of oscillating peristaltic flow through a uniform porous medium

$$(1+\tilde{\lambda}_1^{\alpha}\frac{\partial^{\alpha}}{\partial\tilde{t}^{\alpha}})\tilde{\tau}=\mu\dot{\gamma}, \tag{1}$$

where $\tilde{\lambda}_1, \tilde{t}, \tilde{\tau}, \mu, \dot{\gamma}$ are the relaxation time, time, shear stress, viscosity and rate of shear strain, respectively, and α is a fractional parameter such that $0 \leq \alpha \leq 1$. If $\alpha = 0$, this model reduces to the *classical Newtonian model* and when $\alpha = 1$, the model reduces to the classical Maxwell model. The fractional parameter α characterizes the rheological behavior of material that is intermediate between the Newtonian and Maxwell viscoelastic fluids. This model is composed of a Hooke element connected in series with a Scott–Blair element. The details are given in Mainardi and Spada (2011).

The well-known Darcy law states that, for the flow of a Newtonian fluid through a porous medium, the pressure gradient caused by the friction drag is directly proportional to the velocity. Recently, based on the local volume averaging technique and the balance of forces acting on a volume element of viscoelastic fluids in porous media, Tan and Masuoka (2005a,b, 2007) developed a *modified Darcy-Brinkman model* for flows of some models of viscoelastic fluids in porous media. Darcy resistance quantifies the impedance to the flow in the bulk of the porous space. For generalized Maxwell fluid flows in porous media, the Darcy resistance (Xue and Nie 2008) can be expressed as follows:

$$(1+\tilde{\lambda}_1^{\alpha}\frac{\partial^{\alpha}}{\partial\tilde{t}^{\alpha}})R=-\frac{\mu\varphi}{\tilde{K}}\tilde{u}, \tag{2}$$

where $R, \varphi, \tilde{K}$, and $\tilde{u}$ designate the Darcy resistance, porosity of the porous medium, permeability, and axial velocity, respectively. Figure 1 shows the geometry of oscillating flow through a porous medium, for the present problem.

The constitutive equation for the geometry under consideration (cf. Fig. 1), i.e., oscillating peristaltic flow through a uniform porous medium takes the form:

$$\tilde{h}(\tilde{\xi},\tilde{t})=a-\tilde{\phi}\cos^2\frac{\pi}{\lambda}(\tilde{\xi}-c\tilde{t}), \tag{3}$$

where $\tilde{h}, \lambda, a, c, \tilde{\phi}$ are the transverse oscillating displacement, wavelength, half-width of the channel, wave velocity, and amplitude, respectively.

The governing equations of motion for generalized Maxwell fluid flow through a porous medium using the above formulations can then be shown to take the form:

$$\left.\begin{aligned}\rho\left(\frac{\partial}{\partial\tilde{t}}+\tilde{u}\frac{\partial}{\partial\tilde{\xi}}+\tilde{v}\frac{\partial}{\partial\tilde{\eta}}\right)\tilde{u}&=-\frac{\partial\tilde{p}}{\partial\tilde{\xi}}+\frac{\partial\tilde{\tau}_{\tilde{\xi}\tilde{\xi}}}{\partial\tilde{\xi}}+\frac{\partial\tilde{\tau}_{\tilde{\xi}\tilde{\eta}}}{\partial\tilde{\eta}}+R_{\tilde{\xi}}\\ \rho\left(\frac{\partial}{\partial\tilde{t}}+\tilde{u}\frac{\partial}{\partial\tilde{\xi}}+\tilde{v}\frac{\partial}{\partial\tilde{\eta}}\right)\tilde{v}&=-\frac{\partial\tilde{p}}{\partial\tilde{\eta}}+\frac{\partial\tilde{\tau}_{\tilde{\eta}\tilde{\xi}}}{\partial\tilde{\xi}}+\frac{\partial\tilde{\tau}_{\tilde{\eta}\tilde{\eta}}}{\partial\tilde{\eta}}+R_{\tilde{\eta}}\end{aligned}\right\},\tag{4}$$

where ρ, $\tilde{\xi}$, $\tilde{v}$, $\tilde{\eta}$, $\tilde{p}$, and $R_{\tilde{\xi}}$, $R_{\tilde{\eta}}$ are the fluid density, axial coordinate, transverse velocity, transverse coordinate, pressure, and components of Darcy resistance, respectively.

It is pertinent to introduce the following non-dimensional parameters;

$$\left.\begin{aligned}&\xi=\frac{\tilde{\xi}}{\lambda},\eta=\frac{\tilde{\eta}}{a},t=\frac{c\tilde{t}}{\lambda},\lambda_1=\frac{c\tilde{\lambda}_1}{\lambda},u=\frac{\tilde{u}}{c},v=\frac{\tilde{v}}{c\delta},\phi=\frac{\tilde{\phi}}{a},\delta=\frac{a}{\lambda}\\ &h=\frac{\tilde{h}}{a}=1-\phi\cos^2\pi(\xi-t),p=\frac{\tilde{p}a^2}{\mu c\lambda},\tau=\frac{a\tilde{\tau}}{\mu c},Re=\frac{\rho ca\delta}{\mu},K=\frac{\varphi\tilde{K}}{a^2}\end{aligned}\right\},\tag{5}$$

where δ, Re and K are the wave number, Reynolds number, and permeability parameter, respectively. Substituting the values of shear stress and Darcy resistance from Eqs. (1) and (2) into Eq. (4), using the non-dimensional parameters from Eq. (5) and thereafter applying the long wavelength and low Reynolds number approximations, Eq. (4) reduces to:

$$\left.\begin{aligned}&(1+\lambda_1^{\alpha}\frac{\partial^{\alpha}}{\partial t^{\alpha}})\frac{\partial p}{\partial\xi}=\frac{\partial^2u}{\partial\eta^2}-\frac{u}{K},\\ &\frac{\partial p}{\partial\eta}=0\end{aligned}\right\}.\tag{6}$$

The following boundary and initial conditions are prescribed:

$$\left.\frac{\partial u(\xi,\eta,t)}{\partial\eta}\right|_{\eta=0}=0,\quad u(\xi,\eta,t)|_{\eta=h}=0,\quad \left.\frac{\partial p}{\partial\xi}\right|_{t=0}=0.\tag{7}$$

Integrating Eq. (6) with respect to η and using the first and second condition of Eq. (7), the *axial velocity* is obtained as follows:

$$u=\frac{1}{k^2}\left(1+\lambda_1^{\alpha}\frac{\partial^{\alpha}}{\partial t^{\alpha}}\right)\frac{\partial p}{\partial\xi}\left\{\frac{\cosh(k\eta)}{\cosh(kh)}-1\right\},\tag{8}$$

where $k^2=\frac{1}{K}$.

The volumetric flow rate is defined as $Q=\int_0^h u\mathrm{d}\eta$, which, by virtue of Eq. (8), reduces to

$$Q=\frac{1}{k^3}\left(1+\lambda_1^{\alpha}\frac{\partial^{\alpha}}{\partial t^{\alpha}}\right)\frac{\partial p}{\partial\xi}(\tanh(kh)-kh).\tag{9}$$

The transformations between the wave and the laboratory frames, in dimensionless form, are given by :

$$x=\xi-t,\quad y=\eta,\quad U=u-1,\quad V=v,\tag{10}$$

where the left hand side parameters are in the *wave frame* and the right hand side parameters are in the *laboratory frame*.

Using the transformations defined in Eq. (10), it follows that Eq. (3) can be reduced to

$$h=1-\phi\cos^2(\pi x).\tag{11}$$

The *volumetric flow rate* in the wave frame is given by

$$q = \int_0^h U \mathrm{d}y = \int_0^h (u-1)\mathrm{d}\eta, \tag{12}$$

which, on integration, yields

$$q = Q - h. \tag{13}$$

Averaging the volumetric flow rate along one time period gives

$$\bar{Q} = \int_0^1 Q \mathrm{d}t = \int_0^1 (q+h)\mathrm{d}t, \tag{14}$$

Subsequent integration, yields

$$\bar{Q} = q + 1 - \frac{\phi}{2}. \tag{15}$$

Equation (9), in view of Eq. (15), gives

$$\frac{\partial^\alpha}{\partial t^\alpha}\left(\frac{\partial p}{\partial x}\right) + \frac{1}{\lambda_1^\alpha}\frac{\partial p}{\partial x} = \frac{1}{\lambda_1^\alpha}\frac{k^3\left(\bar{Q}+h-1+\frac{\phi}{2}\right)}{\tanh(kh)-kh}. \tag{16}$$

Using Eqs. (8) and (16), the stream function (ψ) in the wave frame ($U = \frac{\partial \psi}{\partial y}$) is obtained as

$$\psi = \left[\left(\frac{\bar{Q}-1+\frac{\phi}{2}+h}{\tanh(kh)-kh}\right)\left(\frac{\sinh(ky)}{\cosh(kh)} - ky\right) - y\right]. \tag{17}$$

It is evident from Eq. (17) that the stream function is *independent* of fractional parameter and relaxation time.

3 HPM Solutions

Equation (16) can be simplified to yield

$$D_t^\alpha f + \frac{1}{\lambda_1^\alpha} f = -\frac{A}{\lambda_1^\alpha}, \tag{18}$$

where $f(x,t) = \dfrac{\partial p}{\partial x}$ and $A = -\dfrac{k^3\left(\bar{Q}+h-1+\dfrac{\phi}{2}\right)}{\tanh(kh)-kh}$
with the initial condition

$$f(x,0) = 0. \tag{19}$$

According to the HPM given by He (1999), we construct the following homotopy:

$$D_t^\alpha f = -\hat{q}\left[\frac{1}{\lambda_1^\alpha} f + \frac{A}{\lambda_1^\alpha}\right]. \tag{20}$$

Furthermore following (He 1999), we use the homotopy parameter "$\hat{q}$" to expand the solution:

$$f = f_0 + \hat{q} f_1 + \hat{q}^2 f_2 + \hat{q}^3 f_3 + \hat{q}^4 f_4 + \cdots \tag{21}$$

When $\hat{q} \to 1$, Equation (21) becomes the *approximate* solution of Eq. (18). Substituting Eq. (21) in Eq. (20) and comparing the like powers of $\hat{q}$, we obtain the following set of fractional partial differential equations (FPDE):

$$\hat{q}^0 \quad : \quad D_t^\alpha f_0 = 0 \tag{22}$$

$$\hat{q}^1 \quad : \quad D_t^\alpha f_1 = -\frac{1}{\lambda_1^\alpha} f_0 - \frac{A}{\lambda_1^\alpha} \tag{23}$$

$$\hat{q}^2 \quad : \quad D_t^\alpha f_2 = -\frac{1}{\lambda_1^\alpha} f_1 \tag{24}$$

$$\hat{q}^3 \quad : \quad D_t^\alpha f_3 = -\frac{1}{\lambda_1^\alpha} f_2 \tag{25}$$

$$\hat{q}^4 \quad : \quad D_t^\alpha f_4 = -\frac{1}{\lambda_1^\alpha} f_3 \tag{26}$$

and so on.

The method is based on applying the operator J_t^α(the inverse operator of the *Caputo derivative* D_t^α) on both sides of Eqs. (22–26), which leads to:

$$f_0 = 0 \tag{27}$$

$$f_1 = -\frac{A}{\lambda_1^\alpha} \frac{t^\alpha}{\Gamma(\alpha+1)} \tag{28}$$

$$f_2 = \frac{A}{\lambda_1^{2\alpha}} \frac{t^{2\alpha}}{\Gamma(2\alpha+1)} \tag{29}$$

$$f_3 = -\frac{A}{\lambda_1^{3\alpha}} \frac{t^{3\alpha}}{\Gamma(3\alpha+1)} \tag{30}$$

$$f_4 = \frac{A}{\lambda_1^{4\alpha}} \frac{t^{4\alpha}}{\Gamma(4\alpha+1)}. \tag{31}$$

Thus, the exact solution may be obtained as

$$\begin{aligned} f(x,t) &= \sum_{r=0}^{\infty} f_r \\ &= \sum_{r=0}^{\infty} [\psi(\alpha)]^r \frac{t^{r\alpha}}{\Gamma(r\alpha+1)}, \quad \text{where } [\psi(\alpha)]^r = \begin{cases} (-1)^r \frac{A}{\lambda_1^{r\alpha}}, & r \geq 1 \\ 0, & r = 0 \end{cases} \\ &= E_\alpha(\psi(\alpha) t^\alpha), \end{aligned} \tag{32}$$

where $E_\alpha(t) = \sum_{r=0}^{\infty} \frac{t^r}{\Gamma(r\alpha+1)}$, $(\alpha > 0)$ is the *Mittag-Leffler* function in one parameter.

The pressure difference across one wavelength (Δp) and the friction force across one wavelength (F) are defined by the following integrals:

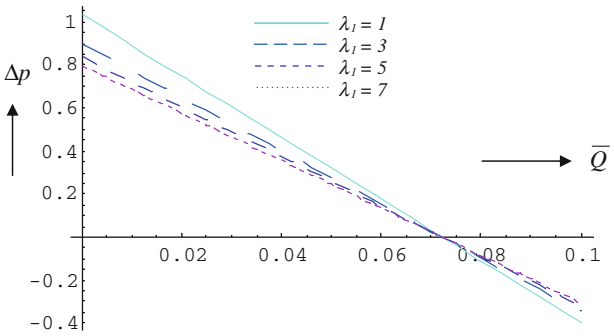

Fig. 2 Pressure versus averaged flow rate for various values of λ_1 at $t = 1, \alpha = 1/4, K = 0.1, \phi = 0.5$

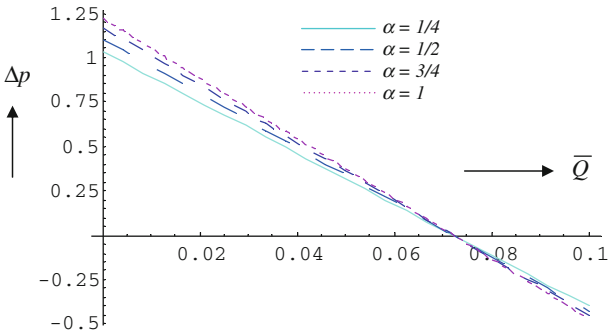

Fig. 3 Pressure versus averaged flow rate for various values of α at $t = 1, K = 0.1, \lambda_1 = 1, \phi = 0.5$

$$\Delta p = \int_0^1 \frac{\partial p}{\partial x} \mathrm{d}x \tag{33}$$

$$F = \int_0^1 h \left(-\frac{\partial p}{\partial x} \right) \mathrm{d}x \tag{34}$$

4 Numerical Results and Discussion

Numerical results have been presented in this section to study the effects of fractional viscoelastic behavior on oscillating peristaltic flow through a uniform porous medium. *Mathematica* software is used to plot all the figures and 100 terms of the *Mittag-Leffler* function have been employed in the computations. All figures have been plotted based on Eqs. (33, 34) and for the integrations, *Simpson's 1/3rd rule* has been implemented. The graphical plots are presented for the effects of relevant values of the control parameters, i.e., the relaxation time (λ_1), fractional parameter (α), and permeability parameter (K) in Figs. 2, 3, 4, 5, 6, 7, and 8.

Figures 2, 3, and 4 illustrate the variation of the volumetric flow rate with pressure gradient for different values of the relaxation time (λ_1), fractional parameter (α), and permeability parameter (K) based on Eq. (33). Different regions on the basis of the values of pressure gradient have been examined in this study. The region for $\Delta p > 0$ is the *entire pumping*

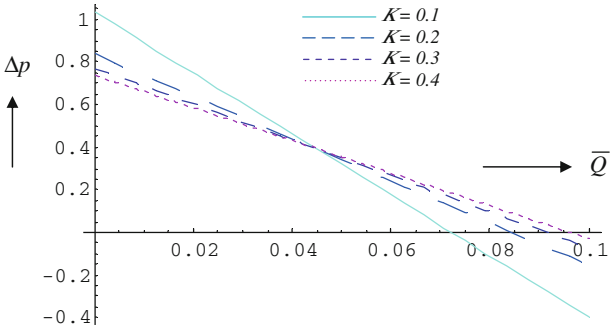

Fig. 4 Pressure versus averaged flow rate for various values of K at $t = 1, \alpha = 1/4, \lambda_1 = 1, \phi = 0.5$

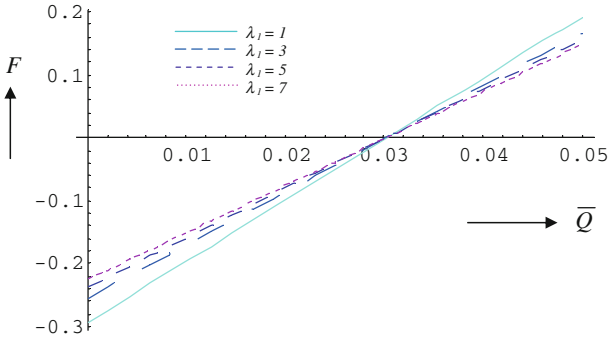

Fig. 5 Frictional force versus averaged flow rate for various values of λ_1 at $t = 1, \alpha = 1/4, K = 0.1, \phi = 0.5$

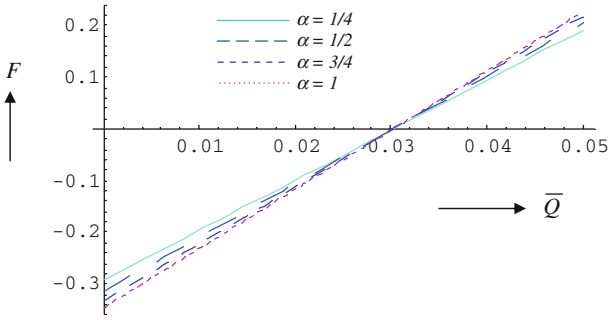

Fig. 6 Frictional force versus averaged flow rate for various values of α at $t = 1, K = 0.1, \lambda_1 = 1, \phi = 0.5$

region, the region for $\Delta p = 0$ is the *free pumping* region, and the region for $\Delta p < 0$ is the *co-pumping* region.

Figure2 shows that in the *entire pumping region*, the volumetric flow rate as well as pressure *decrease* with an *increase* in magnitude of relaxation time; a similar response is computed for the *free pumping region*. However, in the *co-pumping region*, both volumetric flow rate and pressure increase with a rise in magnitude of relaxation time. Inspection of Fig. 2 further reveals that for a *Newtonian fluid* ($\lambda_1 \to 0$), the magnitude of the pressure is greater than that for the Maxwell fluid in the *pumping region* whereas it is markedly less in the *co-pumping* region. Figure 3 indicates that both volumetric flow rate and pressure are

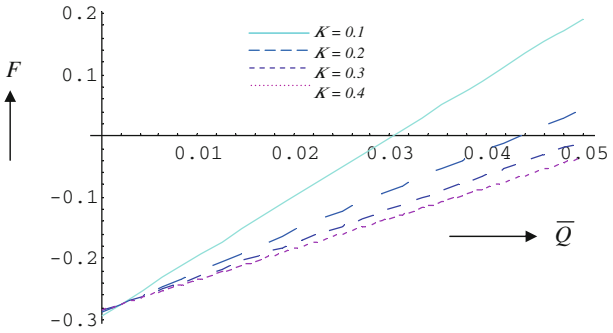

Fig. 7 Frictional force versus averaged flow rate for various values of K at $t = 1, \lambda_1 = 1, \phi = 0.5$

enhanced, both in the pumping region and also in the free pumping region by increasing the magnitude of the fractional parameter. However, the opposite effect is computed for the co-pumping region where both volumetric flow rate and pressure are *depressed* with increasing magnitude of the fractional parameter. It is further observed that for a viscoelastic fluid based on the classical Maxwell model ($\alpha = 1$), the pressure is *greater* than that for viscoelastic fluids with the fractional Maxwell model in the *pumping* region; the reverse trend is apparent in the *co-pumping region*. Figure 4 shows that the pressure diminishes in the pumping region at a critical value of volumetric flow rate and thereafter it increases in the pumping, free pumping, and co-pumping regions with increasing magnitude of permeability parameter. Increasing permeability which corresponds to progressively lesser solid fibers in the porous medium serves to reduce the Darcy resistance. This significantly influences pressures (Zueco et al. 2009a; Rashidi et al. 2011, 2012; Tripathi 2012, 2011h).

Frictional force (F) in the case of the oscillating flow of generalized Maxwell fluids is calculated over *one wave period* in terms of the averaged volumetric flow rate. Figures 5, 6, and 7 show the variation of frictional force with averaged flow rate for different values of the pertinent parameters based on Eq. (34). Figure 5 illustrates that the frictional force is enhanced with increasing relaxation time at a certain value of volumetric flow rate; following this the opposite behavior is observed, i.e., there is a subsequent decrease in frictional force with increasing relaxation time. From Fig. 6, it is observed that the impact of fractional parameter on frictional force is similar in a quantitative sense to that for pressure but opposite in a qualitative sense. The influence of the permeability parameter on frictional force is shown in Fig. 7. This figure indicates that the magnitude of frictional force increases in a very small interval of averaged flow rate and then reduces with increasing magnitude of the permeability parameter. Permeability therefore significantly influences *not only* the pressure distributions (as computed in Fig. 4) *but also* the frictional force in the conduit.

The streamlines on the center-line in the wave frame of reference are found to split to enclose a bolus of fluid particles circulating along closed streamlines under certain conditions. This phenomenon is referred to as *trapping*, which is a characteristic of peristaltic motion. As this bolus appears to be trapped by the wave, the bolus moves with the *same speed* as that of the wave. Figure 8a–g illustrates the streamline patterns and trapping for different values of the permeability parameter and amplitude ratio corresponding to $\bar{Q} = 0.8$ based on Eq. (17). From Fig. 8a–d, it is evident that the size of the trapped bolus increases slightly with increasing magnitude of the permeability parameter (K), i.e., higher permeability aids in the growth of the bolus owing to a simultaneous decrease in Darcian impedance in the porous medium. Increasing permeability is therefore assistive to bolus development and generally

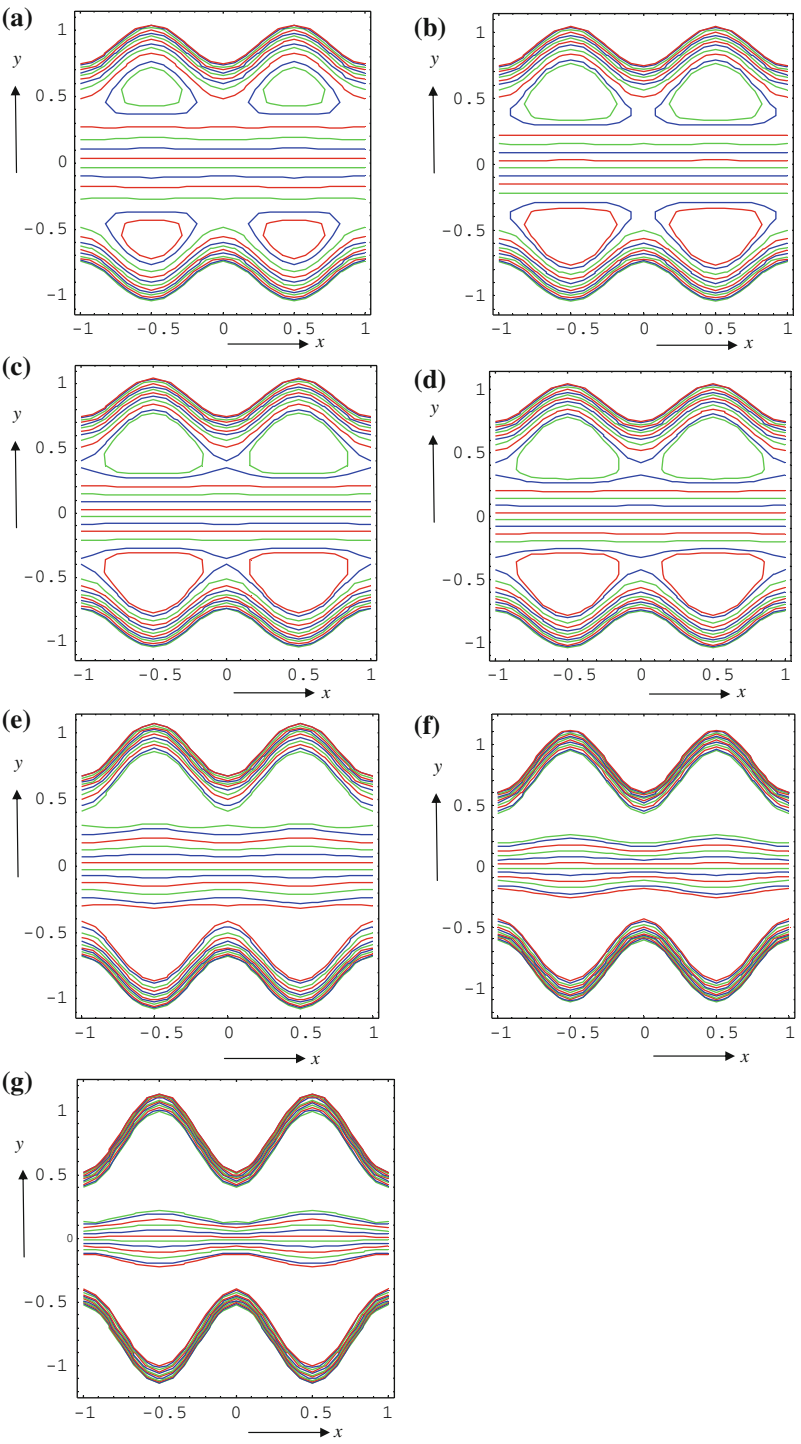

Fig. 8 Streamlines in the wave frame at $\bar{Q} = 0.8$ **a** $\phi = 0.3$, $K = 0.1$, **b** $\phi = 0.3$, $K = 0.2$, **c** $\phi = 0.3$, $K = 0.3$, **d** $\phi = 0.3$, $K = 0.4$, **e** $K = 0.3$, $\phi = 0.4$, **f** $K = 0.3$, $\phi = 0.5$, **g** $K = 0.3$, $\phi = 0.6$

aids flow development also (Zueco et al. 2009b; Bég et al. 1998, 2011). It is further observed that the size of trapped bolus diminishes with an increase in the magnitude of amplitude ratio (ϕ) as illustrated in Fig. 8a, e–g.

5 Conclusions

The influence of viscoelastic behavior, fractional characteristics, and permeability on the flow patterns in two-dimensional oscillating peristaltic non-Newtonian flow in a porous medium, have been studied analytically and numerically. The effects of the key physical parameters on volumetric flow rate, pressure, frictional force, and trapping have been examined. An important observation of the present simulations is that the pressure in the conduit is reduced by increasing the magnitude of relaxation time in the pumping region, whereas it is constant in the free pumping region and enhanced in the co-pumping region. The effect of the fractional parameter on the pressure is opposite to that for relaxation time, in all pumping regions. The present results also reveal that pressure reduces in the pumping region at a *critical value* of volumetric flow rate and subsequently increases in all three regions with a rise in the permeability parameter. The study further shows that the effects of all pertinent parameters on frictional force are quantitatively similar but qualitatively opposite to that of pressure. Furthermore, the present computations show that trapping can be reduced by increasing the amplitude ratio whereas it may be enhanced with increasing the magnitude of the permeability parameter.

References

Bég, O.A., Takhar, H.S., Soundalgekar, V.M.: Thermoconvective flow in a saturated, isotropic, homogeneous porous medium using Brinkman's model: numerical study. Int. J. Numer. Methods Heat Fluid Flow **8**, 559–589 (1998)

Bég, O.A., Zueco, J., Ghosh, S.K.: Unsteady hydromagnetic natural convection of a short-memory viscoelastic fluid in a non-Darcian regime: network simulation. Chem. Eng. Commun. **198**, 172–190 (2011)

He, J.H.: Homotopy perturbation technique. Comput. Meth. Appl. Mech. Eng. **178**, 257–262 (1999)

Khan, M.: The Rayleigh–Stokes problem for an edge in a viscoelastic fluid with a fractional derivative model. Nonlinear Anal. Real World Appl. **10**, 3190–3195 (2009a)

Khan, M.: Exact solutions for the accelerated flows of a generalized second-grade fluid between two sidewalls perpendicular to the plate. J. Porous Media **12**, 919–926 (2009b)

Khan, M., Ali, S.H., Fetecau, H., Qi, C.: Decay of potential vortex for a viscoelastic fluid with fractional Maxwell model. Appl. Math. Model. **33**, 2526–2533 (2009a)

Khan, M., Ali, S.H., Qi, H.: On accelerated flows of a viscoelastic fluid with the fractional Burgers' model. Nonlinear Anal. Real World Appl. **10**, 2286–2296 (2009b)

Khan, M., AliS, H., Qi, H.: Exact solutions of starting flows for a fractional Burgers' fluid between coaxial cylinders. Nonlinear Anal. Real World Appl. **10**, 1775–1783 (2009c)

Khan, M., Anjum, A., Fetecau, H., Qi, C.: Exact solutions for some oscillating motions of a fractional Burgers' fluid. Math. Comput. Modell. **51**, 682–692 (2010)

Liu, Y., Zheng, L., Zhang, X.: Unsteady MHD Couette flow of a generalized Oldroyd-B fluid with fractional derivative. Comput. Math. Appl. **61**, 443–450 (2011)

Mainardi, F., Spada, G.: Creep, relaxation and viscosity properties for basic fractional models in rheology. Eur. Physi. J. Special Top. **193**, 133–160 (2011)

Nadeem, S.: General periodic flows of fractional Oldroyd-B fluid for an edge. Phys. Lett. A **368**, 181–187 (2007)

Qi, H., Jin, H.: Unsteady rotating flows of a viscoelastic fluid with the fractional Maxwell model between coaxial cylinders. Acta Mech. Sin. **22**, 301–305 (2006)

Qi, H., Xu, M.: Some unsteady unidirectional flows of a generalized Oldroyd-B fluid with fractional derivative. Appl. Math. Model. **33**, 4184–4191 (2009)

Rashidi, M.M., Keimanesh, M., Bég, O.A., Hung, T.K.: Magneto-hydrodynamic biorheological transport phenomena in a porous medium: a simulation of magnetic blood flow control and filtration. Int. J. Numer. Methods Biomed. Eng. **27**, 805–821 (2011)

Rashidi, M.M., Bég, O.A., Rahimzadeh, N.: A generalized DTM for combined free and forced convection flow about inclined surfaces in porous media. Chem. Eng. Commun. **199**, 257–282 (2012)
Tan, T., Masuoka, W.C. : Stokes' first problem for a second grade fluid in a porous half-space with heated boundary. Int. J. Non-Linear Mech. **40**, 515–522 (2005a)
Tan, W.C., Masuoka T.: Stokes' first problem for an Oldroyd-B fluid in a porous half space. Phys. Fluids **17**, Article ID 023101 (2005b)
Tan, T., Masuoka, W.C.: Stability analysis of a Maxwell fluid in a porous medium heated from below. Phys. Lett. A **360**, 454–460 (2007)
Tan, W., Pan, M., Xu, W.: A note on unsteady flows of a viscoelastic fluid with the fractional Maxwell model between two parallel plates. Int. J. Non-Linear Mech. **38**, 645–650 (2003)
Tripathi, D.: Numerical study on creeping flow of Burgers' fluids through a peristaltic tube. ASME J. Fluids Eng. **133**, 121104-1-9 (2011a)
Tripathi, D.: A mathematical model for the peristaltic flow of chyme movement in small intestine. Math. Biosci. **233**, 90–97 (2011b)
Tripathi, D.: Peristaltic transport of fractional Maxwell fluids in uniform tubes: application of an endoscope. Comput. Math. Appl. **62**, 1116–1126 (2011c)
Tripathi, D.: Numerical and analytical simulation of peristaltic flows of generalized Oldroyd-B fluids. Int. J. Numer. Methods Fluids **67**, 1932–1943 (2011d)
Tripathi, D.: Numerical study on peristaltic flow of generalized Burgers' fluids in uniform tubes in presence of an endoscope. Int. J. Numer. Methods Biomed. Eng. **27**, 1812–1828 (2011e)
Tripathi, D.: Peristaltic transport of a viscoelastic fluid in a channel. Acta Astron. **68**, 1379–1385 (2011f)
Tripathi, D.: Numerical study on peristaltic transport of fractional bio-fluids. J. Mech. Med. Biol. **11**, 1045–1058 (2011g)
Tripathi, D.: Peristaltic flow of couple-stress conducting fluids through a porous channel: applications to blood flow in the micro-circulatory system. J. Biol. Syst. **19**, 461–477 (2011h)
Tripathi, D.: Peristaltic hemodynamic flow of couple-stress fluids through a porous medium with slip effect. Transp. Porous Media **92**, 559–572 (2012)
Tripathi, D., Pandey, S.K., Das, S.: Peristaltic flow of viscoelastic fluid with fractional Maxwell model through a channel. Appl. Math. Comput. **215**, 3645–3654 (2010)
Tripathi, D., Pandey, S., Das, S.K.: Peristaltic transport of a generalized Burgers' fluid: application to the movement of chyme in small intestine. Acta Astron. **69**, 30–38 (2011)
Vieru, D., Fetecau, C., Fetecau, C.: Flow of a viscoelastic fluid with the fractional Maxwell model between two side walls perpendicular to a plate. Appl. Math. Comput. **200**, 459–464 (2008)
Wang, S., Xu, M.: Axial Couette flow of two kinds of fractional viscoelastic fluids in an annulus. Nonlinear Anal. Real World Appl. **10**, 1087–1096 (2009)
Xue,C., Nie,J.: Exact solutions of Rayleigh–Stokes problem for heated generalized Maxwell fluid in a porous half-space. Math. Prob. Eng. **2008**, Article ID 641431 (2008)
Zueco, J., Bég, O.A., Bég, T.A.: Numerical solutions for unsteady rotating high-porosity medium channel Couette hydrodynamics. Phys. Scr. **80**, 1–8 (2009a)
Zueco, J., Bég, O.A., Bég, T.A., Takhar, H.S.: Numerical study of chemically-reactive buoyancy driven heat and mass transfer across horizontal cylinder in high-porosity non-Darcian regime. J. Porous Media **12**, 519–535 (2009b)